Environmental Earth Sciences (2026) 85:181
https://doi.org/10.1007/s12665-026-12851-2

ORIGINAL ARTICLE

An observational analysis of the urban heat Island in the eastern Mediterranean coast: The case of Thessaloniki, Greece

Evangelos Christakakis[1,2] · **Eirini Aivazidou**[1] · **Erika Brattich**[2]

Received: 16 October 2025 / Accepted: 31 January 2026

Abstract

Urban areas are increasingly affected by rising temperatures and frequent heatwaves (HWs), mainly due to climate change and rapid urbanization. Since the Mediterranean region has been recognized as a climate change hotspot, Thessaloniki, a coastal city in Northern Greece, offers a representative case for exploring the Urban Heat Island (UHI) effect and variability. Based on the hourly surface air temperature data retrieved from a network of stations within five strategically chosen Local Climate Zones (LCZs) during the period 2018–2022, our analysis evaluates the UHI intensity (UHII) and its spatial patterns across areas characterized by different urban morphology. The highest monthly UHII was estimated at 2.1 °C in the urban core. The results revealed a clear UHI spatial gradient across the LCZs, with daily UHII ranging from −2.3 °C to 2.4 °C during daytime and from 0 °C to 2.8 °C at night, with peak intensities observed in summer. Spatiotemporal variations strongly corresponded to each station's LCZ, highlighting the influence of the urban form on the UHI patterns. Comparison of the UHI under HW and non-HW conditions revealed a notable intensification during HW events. Heatwaves were found to amplify the nocturnal UHI intensity by 0.7 to 1.0 °C, most pronounced in dense urban areas, while daytime fluctuations remained minimal. Statistical tests were conducted to ensure robustness and significance of the results. Finally, our study compares the findings with prior research to track the UHI evolution in Thessaloniki and draws parallels with other Mediterranean coastal cities. In synthesis, this work contributes to linking specific urban features to the UHII in a site representative of the Southern European coastal climate. The findings provide guidance for urban planning to improve thermal comfort for urban residents in a climate change hotspot where heatwaves are projected to increase in frequency, intensity and duration.

Keywords Surface air temperature · Urban heat island (UHI) · Heatwaves · Microclimate · Eastern mediterranean coast

Introduction

Rapid urbanization has been amplifying the vulnerability of urban areas to the impacts of global warming and effects of extreme heat risks (Liu et al. 2025). Indeed, nowadays urban areas account for more than 50% of world population (United Nations 2018, 2022), a condition that calls for a comprehensive understanding of the mutual interactions among urbanization, environment, and health. Recent studies suggest that urban overheating can exceed 4–5 °C on average, especially under heat extremes (Santamouris 2020). Notably, as global temperatures approach the 1.5 °C climate threshold (IPCC 2023), the urban heat island (UHI) effect, a phenomenon where surface air temperatures in cities are notably higher than in their surrounding rural and suburban areas (Oke 1973), has been shown to amplify heatwave (HW) temperatures by up to 8.5 °C (Pappalardo et al. 2023). This phenomenon further generates ramifications in the local economies in terms of intensified energy demand (Giannakopoulos et al. 2016), potentially resulting in poor power plant efficiency (Santamouris 2020). In addition, the higher temperatures in the cities increase thermal stress, leading to both direct (e.g., increased death rates) and indirect (e.g., sleep disorders, respiratory problems) effects on human health (Arifwidodo et al. 2019).

✉ Evangelos Christakakis
evangelos.christakakis@unibo.it

[1] Department of Industrial Engineering and Management, International Hellenic University (IHU), Thessaloniki 57400, Greece

[2] Department of Physics and Astronomy "Augusto Righi", University of Bologna (UNIBO), Bologna 40126, Italy

As buildings have the ability to absorb energy and emit radiation back to the environment, they tend to increase the temperature of the urban landscape, while the lack of required distance between them may not allow for the proper wind circulation (Voogt and Oke 2003). At the same time, the high intensity of anthropogenic activities, including urban transportation (e.g., use of internal combustion engines) and residential heating, can reinforce the UHI phenomenon as the produced CO_2 emissions increase air temperatures (Nuruzzaman 2015; Silva et al. 2022). Moreover, the lack of green spaces which often characterizes the city centers limits the evapotranspiration process which, in turn, worsens the UHI intensity (UHII) (Oke 1982).

Focusing on the coastal Mediterranean region, a well-known climate change hotspot (e.g., Lazoglou et al. 2024), several UHI studies have been conducted, for example in the cities of Valencia and Barcelona (Spain), Bari and Rome (Italy), and Athens (Greece). In particular, the maximum nocturnal UHI based on air temperature in Valencia reached 2.3 ℃ after the hottest day recorded in the study period (Lehoczky et al. 2017), whereas the highest UHI in Barcelona reached 4.3 ℃ in summer (Salvati et al. 2017; Martin-Vide And Moreno-Garcia 2020). Similarly, the high-density areas in Bari recorded high UHI values both during daytime (4 ℃) and nighttime (4.2 ℃) (Martinelli et al. 2020). Rome experiences distinct seasonal variations in the UHII, with winter UHI ranging between 1.6 °C and 2.8 °C and summer UHI peaking between 2.2 °C and 3.0° (Keppas et al. 2021). Finally, Athens demonstrates higher UHIIs intensities than its surroundings during night (>4 ℃), while lower UHI values are registered during early morning and mid-day hours (Giannaros et al. 2013).

Beyond city-specific values, comparative research on Mediterranean cities, such as Rome, Bari, Athens, and Crete, highlights distinctive mechanisms shaping UHI dynamics (Giannaros et al. 2013; Lazoglou et al. 2024). The proximity of the sea introduces cooling sea-breeze circulations that mitigate daytime UHII, while the thermal inertia of water bodies reinforces nocturnal heat retention. Irregular coastal morphology and compact urban forms further amplify spatial variability, and seasonal contrasts are particularly strong, with enhanced UHIs during summer HWs but weaker effects in cooler months (Martinelli et al. 2020; Di Bernardino et al. 2023). However, despite this growing body of work, most studies have focused on western or central Mediterranean settings, while long-term analyses of the UHI intensity and variability in the eastern Mediterranean remain scarce. In particular, the temporal evolution of UHIs under recurrent HW conditions, as well as systematic comparisons across different coastal morphologies, are still insufficiently explored. By situating Thessaloniki within this comparative framework, the present study explicitly investigates how coastal influences interact with the city's topography and urban morphology, while also assessing the spatiotemporal variability of UHI during HW events and its long-term evolution providing updated observational evidence from one of the easternmost Mediterranean urban centers.

In this context, this paper aims to provide an elaborate analysis on the UHI effect in the urban area of Thessaloniki, Greece, offering meaningful insights about the impact of the built environment and human activities on the urban microclimate in the eastern Mediterranean Sea. In particular, Thessaloniki's distinct topography is characterized by its coastal location, irregular street patterns, and mixed urban morphology, which can contribute uniquely to the spatial variability of the UHI effect (Liu et al. 2023). Unlike more uniformly planned cities, Thessaloniki's complex terrain and urban form influence wind flow, solar exposure, and heat retention, rendering its UHI patterns notably different that call for further analysis (Li et al. 2020). To this end, this work aims to respond to the following research questions (RQs):

- RQ#1 – How strong and spatiotemporally variable is the UHII in Thessaloniki, and which is the impact of local HW events?
- RQ#2 – How has the UHI evolved in Thessaloniki, and which are the similarities with other Mediterranean coastal cities?

To respond to the RQs, we employ an acknowledged methodological approach for quantifying Thessaloniki's UHII (i.e., hourly, monthly, yearly, daytime/nocturnal) based on the surface air temperature data recorded at five (5) urban weather stations (diversified in terms of geospatial characteristics) during the period 2018–2022. Notably, this research is anticipated to deliver updated UHI outcomes in Thessaloniki to explore the impact of climate change on the phenomenon over the years, compared to the former findings for the same city (Giannaros And Melas 2012). In addition, as the local urban morphology, microclimate, and meteorological conditions can modulate the extent to which UHI exacerbates heat stress during HW events (Possega et al. 2022), our study further aims to analyze the complex interactions between HWs and the UHI phenomenon in Thessaloniki. Finally, a comparative analysis with recent studies in other coastal Mediterranean cities investigates existing similarities, providing common inferences and proposed measures to alleviate the UHI intensity in the region under study. Although numerous studies have examined the UHI effect in Mediterranean cities, important gaps remain, particularly for coastal cities in the eastern Mediterranean. Evidence from multi-year analyses is still limited, while the combined influence of urban morphology -using the Local Climate Zone (LCZ) framework- and proximity to the sea on the UHI intensity and its spatial and temporal variability have not been sufficiently explored. In addition, despite the Mediterranean basin being a recognized climate-change hotspot, the interaction between HW and the UHI effect remains poorly documented in this region.

While the methodological approach of this study aligns with previous research on UHIs, our work offers novel contributions beyond its geographic focus. Specifically, it provides an elaborate evaluation of the influence of LCZs on the UHII, along with an assessment of HW-UHI interactions, with particular focus on nighttime conditions. Overall, this work contributes to the urban microclimate research field by shedding light on the surface weather conditions of an eastern Mediterranean coastal city by providing up-to-date UHI calculations to support informed decision-making for sustainable urbanism. The remainder of this paper is structured as follows. In Materials and methods section , detailed descriptions of the study area, the data collection process, and the methodological approach are provided. The Results section analyses the UHI patterns in the city of Thessaloniki and the HWs' effect on UHI, along with a juxtaposition with previous studies in the coastal Mediterranean region. Finally the Discussion and conclusions section ends with a discussion on the implications and the associated policy recommendations for mitigating the UHI effect.

Materials and methods

In this section, we first describe the geographical and climatic characteristics of Thessaloniki as the basis of our analysis. We then present the network of meteorological stations used for surface air temperature monitoring and detail the data collection and preprocessing procedures. Finally, we outline the methodological framework applied to assess UHII and identify any HW events.

Study area, identification of meteorological stations, and data collection

The study was carried out in the city of Thessaloniki (40.64 N, 22.94 E, Central Macedonia Region, Greece), located in the northern coast of the Aegean Sea. The urban area of Thessaloniki has a high population density, hosting approximately 820,000 inhabitants in 2021 (Hellenic Statistical Authority 2023). Concerning its urban climate, Thessaloniki is considered a Mediterranean coastal city with mild winters and hot and moderately dry summers (Giannaros And Melas 2012). The highest temperatures are recorded in July (mean daily maximum temperature at 31.5 ℃) and the lowest ones in January (mean daily minimum temperature at 1.3 ℃), while there are approximately 32 days of frost per year. The mean annual rainfall is 449 mm, distributed over 114 days on average, with a distinct minimum in summer and a broad peak from Autumn through Spring, reaching its maximum in Winter. November and December are the wettest months and August the driest (World Meteorological Organization 2023). The annual average relative humidity is 66.5%, with a minimum of 52.7% in July and a maximum of around 77% in November and December (Hellenic National Meteorological Service 2023). Regarding extreme weather conditions, Thessaloniki has seen a sharp rise in HW frequency, with 56 events recorded between 1950 and 2020, 75% of which occurred after 1990. Their frequency increased by 72% in recent decades (+0.3 events/decade), peaking in 2012. Most HW days occur in July (39%) and August (38%), while durations of summer heat waves lengthened significantly (+0.4 days/decade), reaching 12 days in 2017 (Galanaki et al. 2023).

The analysis was performed under the urban canopy layer (i.e., beneath the height of buildings) and it is based on surface air temperature data recorded in six (6) fixed meteorological stations. Specifically, five (5) weather stations are located in the urban area of Thessaloniki and a reference station (used as baseline) in the suburban airport area (Fig. 1). Regarding the urban weather stations, two of them (Stations

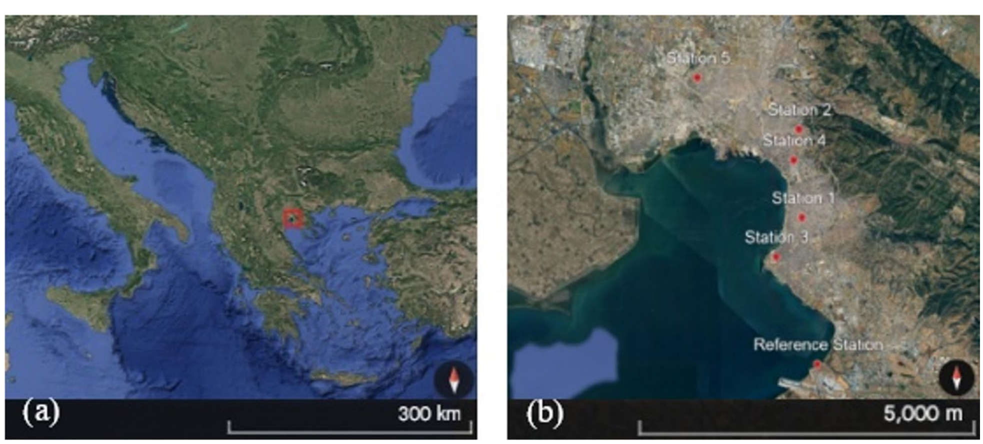

Fig. 1 Geographic location of Thessaloniki (left, red box) and the location of the weather stations (right, red markers). Note: A scale bar and a compass are included.(Source: Google Earth)

1–2) are managed by the department of Environment and Climate Change Adaption of the Municipality of Thessaloniki, while the remaining three (Stations 3–5) are controlled by the National Observatory of Athens. Finally, the reference station is located at the International Airport of Thessaloniki in the Municipality of Thermi (suburban area) and managed by the Hellenic National Meteorological Service. Notably, the selection of the reference station was done in agreement with all the requirements defined by literature (e.g., Martinelli et al. 2020; Acero et al. 2013; Giannaros And Melas 2012; Anjos and Lopes 2017; Santamouris et al. 2017; Yun et al. 2020), namely suggesting considering sites poorly influenced by the presence of surrounding buildings and by a higher amount of vegetation. Considering also the availability of weather data from local authorities, Thessaloniki's airport station was chosen as the reference suburban station for this work.

The spatial representativeness of the monitoring network was evaluated using the Local Climate Zone (LCZ) classification of Thessaloniki (Fig. 2). The urban area is dominated by LCZ 1 (compact mid-rise), LCZ 2 (compact low-rise), and LCZ 8 (large low-rise). The five urban stations fall within LCZs 2, 6, and 8, capturing the main morphological types. Minor LCZs (e.g., LCZ 3 or 5) are not represented but occupy only a small fraction of the city and have minimal influence on overall UHI patterns. Due to the limited number and uneven distribution of stations, a thermal gradient map could not be produced; instead, Fig. 2 shows the LCZ distribution, providing context for the relationship between urban morphology and temperature. Overall, the selected stations adequately cover the dominant LCZs for assessing Thessaloniki's UHI.

In more detail, following the spatial context used in the study of Giannaros and Melas (2012) who employed similar station locations in the same city, the reference station was selected in a non-residential, obstruction-free area near the sea, corresponding to LCZ 9 (Sparsely built) with subclass G (Water). Stations 1, 3, and 5 lie within the city's dense urban core, characterized by mid-rise residential buildings, narrow streets, and minimal green space, which is typical of LCZ 2 (Compact midrise). Station 2 is in a mainly residential zone with low-rise buildings and some green areas, fitting LCZ 6 (Open low-rise). Station 4, situated in the central exhibition area, features large, low-rise structures on paved surfaces with little vegetation, aligning with LCZ 8 (Large low-rise). Table 1 summarizes the characteristics of the weather stations used in this work.

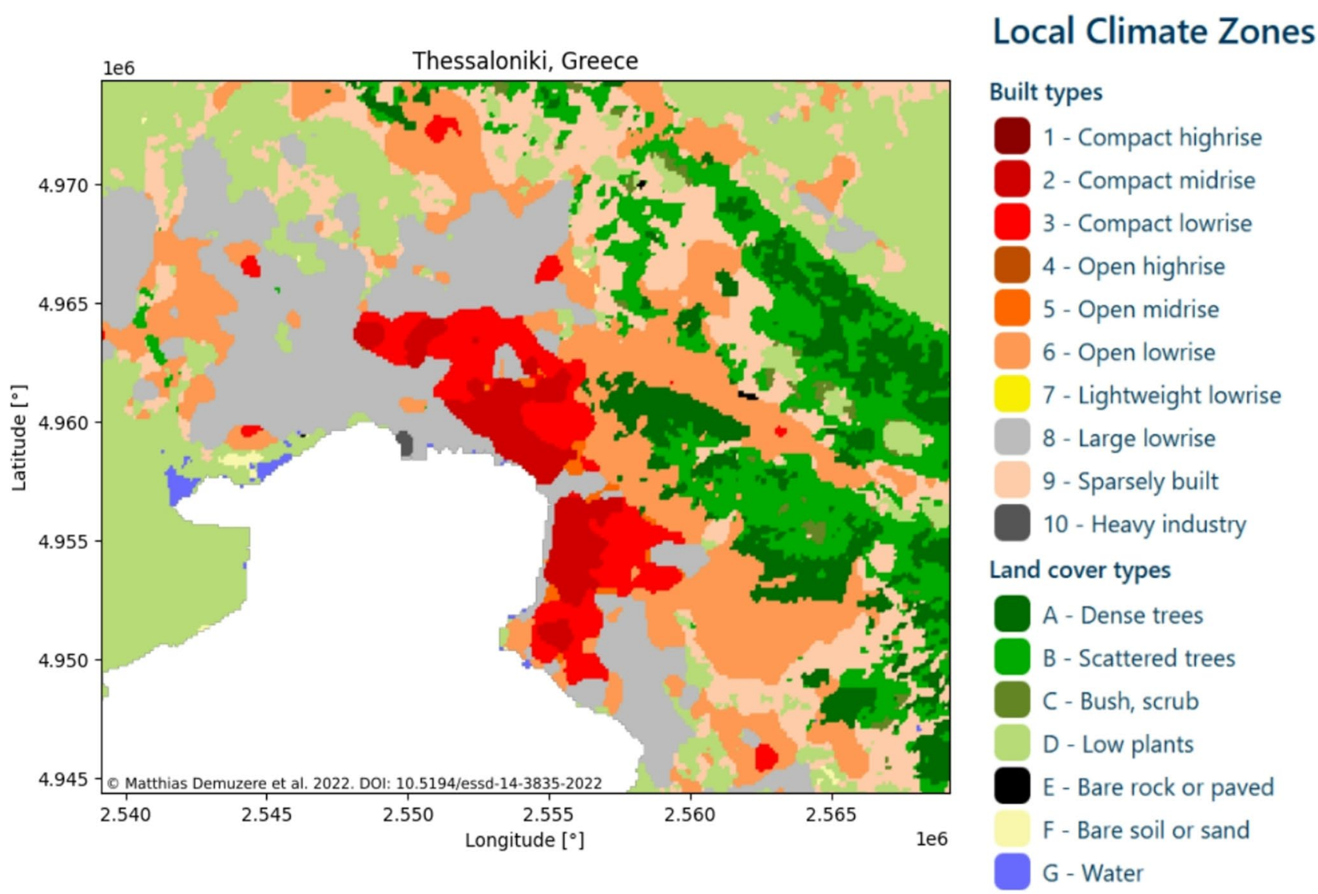

Fig. 2 Local Climate Zones (LCZs) map of Thessaloniki

Table 1 Site characteristics of the weather stations under study (Images' source: Google Earth)

Station ID	Station name and abbrevation	Data source	Longitude (degrees east)	Latitude (degrees north)	Elevation (m)	Local Climatic Zone (LCZ)	Map Location
Reference	Thessaloniki Airport (SKG)	Hellenic National Meteorological Service	22° 58' 12.0"	40° 31' 48.0"	2	LCZ 9_G (Sparsely built - Water)	
1	25 Martiou (MRT)	Department of Environment and Climate Change Adaption / Municipality of Thessaloniki	22° 57' 38.1"	40° 36' 04.6"	20	LCZ 2 (Compact midrise)	
2	Eptapyrgio (EPG)	Department of Environment and Climate Change Adaption / Municipality of Thessaloniki	22° 57' 30.4"	40° 38' 39.3"	183	LCZ 6 (Open low-rise)	
3	Kalamaria (KLM)	National Observatory of Athens	22° 56' 39.0"	40° 34' 56.0"	33	LCZ 2 (Compact midrise)	
4	Thessaloniki's Fair Center (HXP)	National Observatory of Athens	22° 57' 19.1"	40° 37' 45.4"	39	LCZ 8 (Large low-rise)	
5	Kordelio (KRD)	National Observatory of Athens	22° 53' 39.0"	40° 40' 10.7"	24	LCZ 2 (Compact midrise)	

A five-year period (from January 2018 to December 2022) is used for the analysis. This period was selected as it provides a recent, continuous, and methodologically consistent multi-year record that captures both typical climatic conditions and several documented HWs, enabling a robust evaluation of UHI behavior under average and extreme thermal stress. Furthermore, 2018–2022 is the only interval in which high-quality homogeneous hourly temperature data were available across all monitoring stations, whereas extending this record was limited by data gaps and inconsistencies. The hourly data of the surface air temperatures were provided by the managerial authorities of the weather stations. The necessary meteorological data were collected to analyze the most recent (and available) air temperature dynamics in the city of Thessaloniki. During the five-year time frame, some periods without data records were identified, probably due to technical malfunctions or temporary lack of stewardship. To avoid introducing bias, missing data were neither estimated nor interpolated, as doing so would involve assigning arbitrary values. Table 2 presents the annual percentages of missing hourly air temperature data for each monitoring station. Nevertheless, data validation and cleaning were performed before

Table 2 Percentage (%) of missing data for each station from 2018 to 2022

Station	2018	2019	2020	2021	2022
Reference Station (SKG)	3.3%	7.3%	0.5%	0.7%	1.2%
Station 1(MRT)	0%	4.3%	0.2%	0%	0%
Station 2 (EPG)	1.2%	0%	6.9%	10.3%	29.3%
Station 3 (KLM)	100%	100%	100%	30.3%	0%
Station 4 (HXP)	67.2%	0%	0.1%	0%	0%
Station 5 (KRD)	35.5%	0%	0%	0%	0%

processing the data. In case individual values were missing, inconsistent, or unrealistic (e.g., winter temperature value over 35 ℃), manual preprocessing was conducted to limit the presence of errors in our analysis. Finally, based on the hourly temperature data collected, the daily, monthly, and annual time average series have been further calculated.

Methodological approach

The variation in air temperature within a city environment can be studied by comparing urban stations with a reference suburban station that shares similar topographic features, such as elevation (Giannaros And Melas 2012). In principle, the urban area coincides with the core of a city, which is densely populated, while the suburban area refers to locations outside of the core of the city that are less densely populated (Martinelli et al. 2020). For this study, the airport station was selected as the suburban reference. This choice was based on the availability of a long-term, continuous, and high-quality dataset for the entire study period, whereas alternative locations have substantial data gaps. Its use is also supported by previous UHI studies (e.g. Giannaros And Melas 2012). According to Kim and Baik (2005), the UHI intensity (UHII) can be defined as the difference in air temperature between the urban and the surrounding suburban/rural area. Thus, the **UHII** can be calculated as:

$$UHI = T_u(i) - T_r$$

where $\mathbf{T_u(i)}$ is the temperature of the i-th urban station and $\mathbf{T_r}$ is the temperature of the suburban station.

To evaluate the UHI phenomenon comprehensively, the UHII was analyzed across multiple temporal scales: hourly ($UHII_h$), monthly ($UHII_m$), annual ($UHII_y$), daytime ($UHII_{day}$), and nocturnal ($UHII_{night}$). For all scales, the air temperature difference between each urban station (Stations 1–5) and the reference station during the five-year period was calculated using the UHII equation. The hourly UHII ($\mathbf{UHII_h}$) was directly calculated based on the retrieved air temperature data, with separate analyses conducted for the coldest (January) and hottest (July) periods (i.e., extreme temperature months). The monthly ($\mathbf{UHII_m}$) and annual ($\mathbf{UHII_y}$) averages were derived by aggregating hourly data into mean values for each station, compared with the respective reference station mean temperatures. Similarly, to obtain the daytime ($\mathbf{UHII_{day}}$) and nocturnal ($\mathbf{UHII_{night}}$) values, daytime (07:00–18:59, local time) and nighttime (19:00–06:59, local time) temperature averages were calculated on a monthly basis.

To evaluate the behavior and variability of the UHI during HW events, HW periods were identified using the approach developed by Perkins and Alexander (2013) based on the combination of two thresholds, i.e. the 90th percentiles of minimum (CTN90pct) and maximum (CTX90pct) daily temperatures. Basically, the CTN90pct-based method identifies HWs when the minimum daily temperature exceeds the 90th percentile for at least three consecutive days. Similarly, the CTX90pct method defines a HW when the maximum daily temperature surpasses the 90th percentile for a minimum of three consecutive days. In this study, the percentiles were computed for each calendar day using a 15-day running window centered on the day of interest, based on the 1981–2010 climatological reference period. The climatological thresholds were calculated exclusively from the long-term dataset of the reference station adopted in this study (same coordinates and metadata), thereby providing a consistent baseline for HW identification. Heatwave detection was applied year-round using the Hotspell Python package. Consequently, the comparison of the UHII between HW and non-HW days includes all heatwave events occurring throughout the 2018–2022 study period, without restriction to specific months or seasons. Then, the UHII during HW and non-HW days was compared across the five selected stations for the whole study period. The results consider both daytime and nocturnal UHII. From a technical perspective, all data processing and analyses were performed computationally using Python (3.12) with NumPy and Pandas libraries for statistical operations and Matplotlib for visualization. MATLAB (R2024b) was employed for initial data alignment and quality control.

Finally, statistical analyses were performed to provide quantitative support for the interpretation of the results. Differences in the UHII between heatwave HW and non-HW days were evaluated using the non-parametric Mann–Whitney U test. Temporal trends in the UHII over the 2018–2022 period were assessed using the Mann–Kendall trend test. In addition, the relationship between the UHII and background air temperature was examined at the monthly scale using Pearson correlation. All tests were two-sided with a significance level of α=0.05.

Analyses were conducted in Python using pandas, NumPy, SciPy, and the Hotspell package, with temperature data aggregated to daily or monthly values as appropriate. Figure 3 illustrates the complete methodological framework followed in our analysis, as described in Materials and methods section.

Meteorological data analysis: the case of Thessaloniki, Greece

In this section, we present a detailed analysis of meteorological data from Thessaloniki, Greece, focusing on air temperature variations across different urban LCZs. We then quantify the UHII based hourly, monthly, and daytime/nocturnal calculations, further investigating its interaction with HW events using the above-described percentile-based identification methods. Finally, we compare our findings with previous studies to contextualize urban microclimate dynamics and identify any knowledge gaps for future research and urban planning purposes.

Fundamental analysis of air temperature data series

The analysis initially identifies the hourly variations in the air temperature patterns across the six stations (including the reference one). The hourly temperatures collected over the five-year period are then described based on a statistical evaluation (box plot analysis; Fig. 4). Notably, Station 3 (LCZ 2) recorded the highest average air temperature (18.4 °C), followed by Station 5 (LCZ 2, 18.3 °C) and Station 2 (LCZ 6, 17.1 °C), while the reference station (LCZ 9_G) reported the lowest one (16.5 °C). Station 5 also registered the absolute highest temperature (42.5 °C), and the reference station corresponds to the absolute lowest (−8 °C). Throughout the five-year period, all five urban stations consistently recorded temperatures above −6 °C. These differences align with the stations' Local Climate Zones: LCZ 2 sites (Stations 3 and 5) are dense, built-up areas that retain heat, whereas LCZ 9_G (reference station) is sparsely built and more exposed, allowing for greater cooling. The box plot shows that Station 5 had the widest value dispersion (13.4 °C, Interquartile range; IQR), likely due to microclimatic variability, while Stations 2 (LCZ 6) and 3 (LCZ 2) showed the least variability (12.9 °C, IQR), indicating more thermally consistent settings. This pattern highlights the significant influence of LCZs on the UHII, with denser, built-up areas (LCZ 2) exhibiting higher and more variable temperatures due to greater heat retention, while more open vegetated zones (LCZ 9_G) experience lower temperatures and enhanced cooling effects.

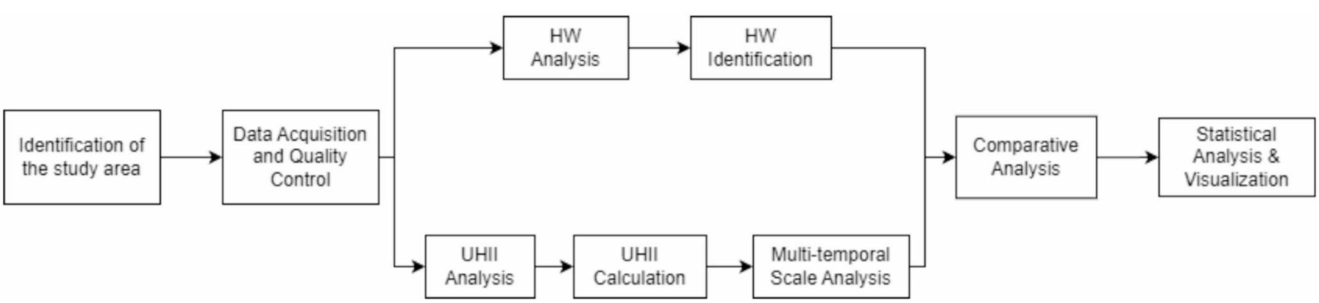

Fig. 3 Schematic overview of the methodological framework used in the case study

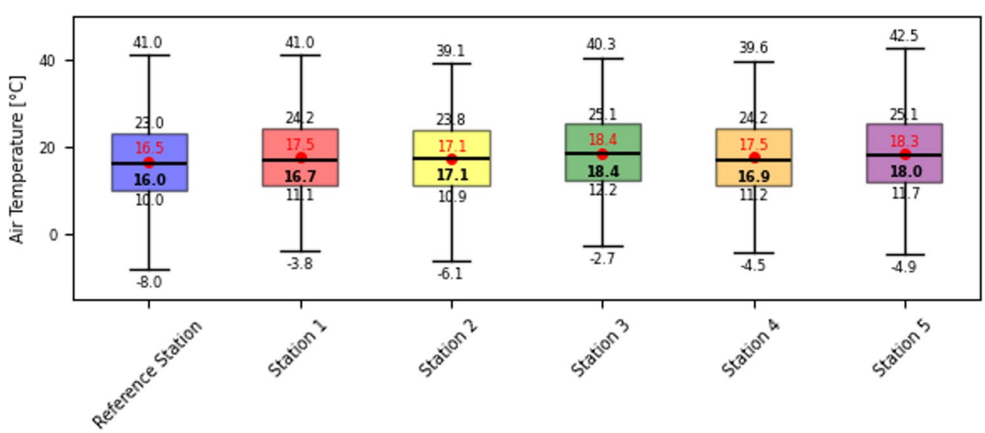

Fig. 4 Box plot analysis of the hourly atmospheric temperatures recorded at each station. Boxes enclose the interquartile range (IQR), spanning from the 25th to 75th percentile. Horizontal lines inside each box indicate the median, with the corresponding value displayed in black, while whiskers extend to the minimum and maximum values within 1.5 times the IQR. Red dots represent the mean values, with the corresponding value displayed in red

After that, a detailed hourly analysis of the air temperatures observed at each station was performed (Fig. 5). This involved plotting the hourly air temperature data series for both the hottest month (July) and the coldest month (January) across the five-year period (Fig. 4). Notably, the lowest temperatures are identified at the Reference Station (Airport) both for the coldest (January) and hottest (July) periods, followed by Station 2. These findings align with the stations' LCZ classifications. The Reference Station is situated in the LCZ 9 (i.e., sparsely built, coastal suburban area with low-rise development and abundant permeable surfaces), which typically exhibits lower temperatures due to reduced heat retention and higher ventilation. At the same time, Station 2, located in an area classified as LCZ 6 (open low-rise with scattered vegetation and greener areas), also shows cooler temperatures compared to denser urban stations, as the elevation, lower building density, and higher vegetation cover promote enhanced cooling effects. In contrast, the warmer urban stations belong to more built-up LCZs (e.g., compact mid-rise) including Stations 1,3 and 5, where materials and urban morphology exacerbate heat retention. In addition, the hourly air temperature in July exhibits greater variability and a larger diurnal temperature range than in January.

Figure 6 illustrates the monthly temperature trends, displaying the average, highest, and lowest recorded temperatures for each of the six locations over the five-year period. The highest average monthly values are recorded in Stations 5 and 1 (29.6 °C in July 2021 and 29.1 °C in August 2021, respectively), and the lowest ones are observed in Station 2 (4.5 °C in January 2021). Station 2 shows the lowest range in monthly averages. These variations can be partly explained by LCZ classification. Stations 1, 3, and 5, located in LCZ 2 (Compact midrise), experience higher temperatures due to dense built-up areas and limited vegetation. Station 2, in LCZ 6 (Open low-rise), records lower temperatures, likely due to the presence of more green spaces and lower building density. The reference station (LCZ 9_G; near water) consistently shows the coolest observations, reflecting minimal urban influence and the moderating effect of the nearby sea.

Looking at the patterns of the maximum monthly air temperatures, Stations 3 and 5 show the highest values, whereas Station 2 exhibits the lowest values. In particular, during the coldest months, the highest maximum temperatures are recorded at Stations 2, 4, and 5, while the lowest maximum values are recorded at the Reference Station and Station 3. For the hottest months, the monthly maximum temperature values show a relatively smaller variation for all six weather stations. In terms of the minimum temperatures, the Reference Station records the lowest temperatures in both hot and cold months. Notably, the minimum temperature difference between the Reference Station and the remaining stations is particularly evident in the cold months of winter (from December to February). Overall, these findings align with expectations, considering the location of the Reference Station in a suburban costal area strongly impacted by the sea breeze phenomenon (Di Bernardino et al. 2023) and therefore displaying the lowest minimum temperatures, and the one of Station 2 in a less urbanized and higher altitude area.

Urban heat Island intensity

The analyses conducted so far suggest the presence of a spatially variable UHI phenomenon in the area of Thessaloniki. In this subsection, the most acknowledged indicator to quantitatively describe the UHI effect, namely the UHII, is studied. The analysis is performed considering: (i) the hourly air temperature, (ii) the monthly average and annual average air temperature, and (iii) the daily average air temperature (i.e., daytime and nocturnal).

Hourly urban heat Island intensity during the extreme temperature periods

The analysis of the $UHII_h$ pattern was based on the hourly air temperature differences between each station and the reference one for the years 2018–2022. Here, we have decided to focus deeper on the months of January and July, as they represent the coldest and hottest months of the year based on our dataset, with average daily temperatures around 8 °C and 28 °C, respectively. By examining these two opposite months, we can better understand the seasonal variability of UHI and its underlying drivers. Based on the equation proposed by Kim and Baik (2005), the air temperature difference between each station (Stations 1–5) and the Reference Station was calculated on an hourly basis (Fig. 7).

Upon examining the hourly outcomes, we can observe that the $UHII_h$ in July (hottest month) is higher than that in January (coldest month) in all five years examined. In addition, it is evident that the $UHII_h$ is higher during night hours in contrast to the middle of the day when we can even detect negative values (i.e., Reference Station temperatures are higher than those of the rest). This diurnal pattern is well-documented in urban climatology and can be attributed to the thermal properties of urban materials and land cover. At night, the slow release of heat stored in built-up surfaces (e.g., concrete, asphalt) maintains warmer urban temperatures, while rural areas cool more rapidly due to higher radiative losses and lower thermal inertia (Vardoulakis et al. 2013). Moreover, this effect can be attributed to the low solar altitude and the trapping of cold air within densely built and high-rise urban areas, where limited sky exposure and narrow street canyons hinder heat dissipation (Giridharan And Kolokotroni 2009). In addition, the UHI phenomenon is more frequent during the

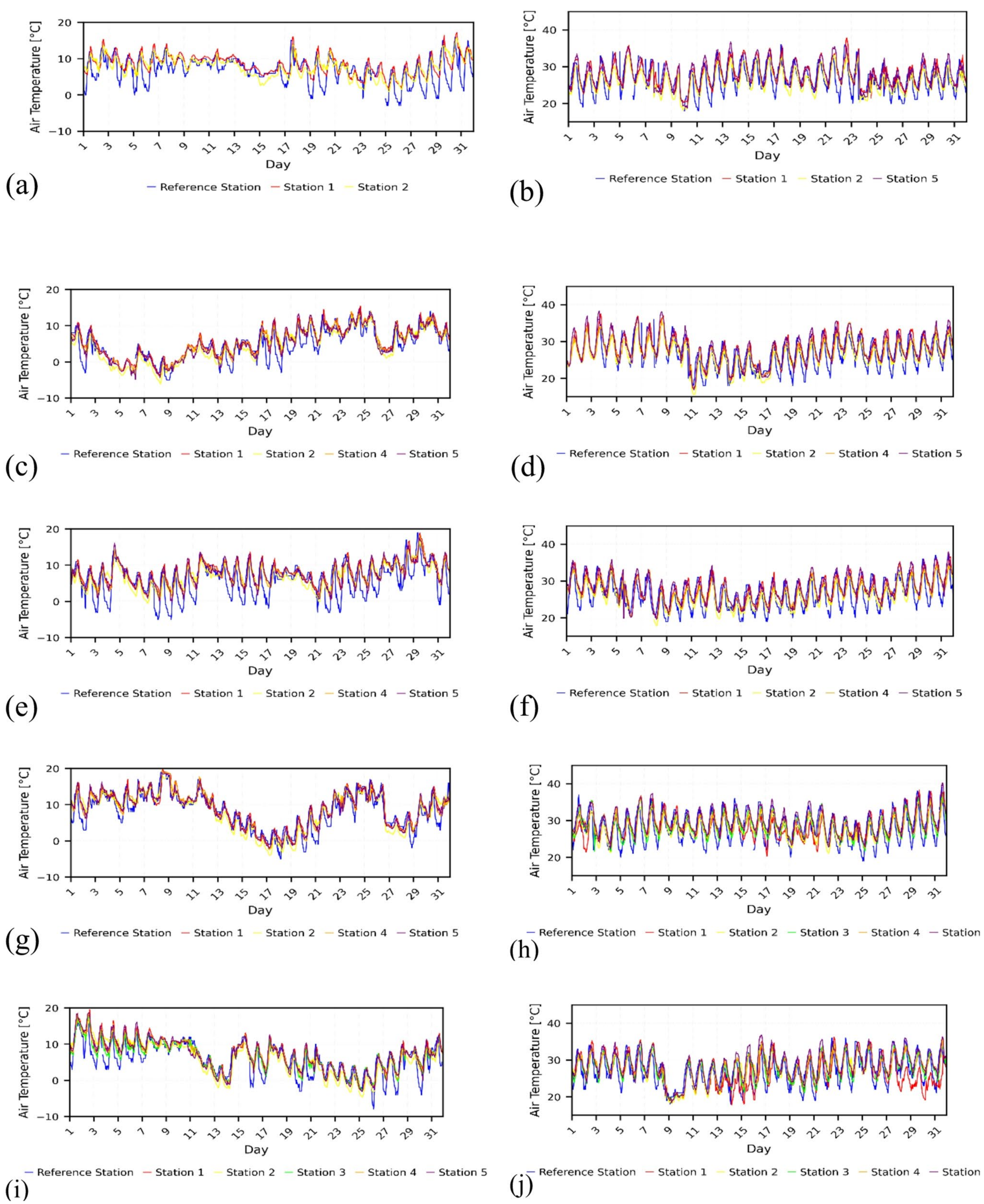

Fig. 5 Hourly air temperatures in January (left) and July (right) from 2018 (top) to 2022 (bottom) at the different meteorological stations in Thessaloniki, Greece

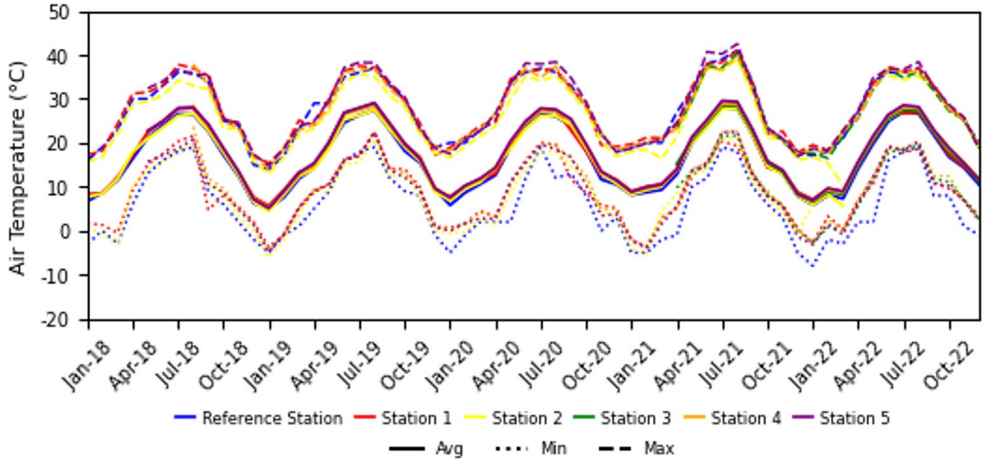

Fig. 6 Monthly average (solid line), minimum (dotted line) and maximum (dashed) air temperatures during 2018–2022 at the different meteorological stations in Thessaloniki, Greece

hottest month (July) than in the coldest one (January); consequently, a noticeable "cold island effect" manifests in specific areas of the urban area (i.e., Station 2 and 4) during the winter season. This phenomenon occurs as urban materials retain and re-radiate heat more efficiently in summer, while in winter (Lu et al. 2024), the lack of vegetation and reduced solar exposure can lead to localized cooling in certain zones (Bouketta 2023). The cold island effect is also documented in the literature, where factors like wind patterns, shading, and anthropogenic heat variations contribute to temperature dips in specific urban zones (An et al. 2020).

Average monthly and annual urban heat Island intensities

In Fig. 8, the $UHII_m$ series (Analytic data are provided in Table A1 of the Appendix) is presented. It should be noted that there was no available data for the months of March, April and May during the year 2022 at Station 2, due to potential maintenance or malfunction. In addition, the data retrieved from Stations 3, 4, and 5 start from the month that they were installed and onwards. For the $UHII_m$ calculation to avoid bias and ensure the reliability of the results, missing air temperature data were excluded, while no data imputation was performed. In addition, performing a Mann–Kendall trend analysis of the UHII indicated no statistically significant long-term trends at any of the five stations during the study period (all $p > 0.05$, Tau between −0.16 and 0.22). The slope of the UHII change was minimal across all stations, suggesting that the UHII remained stable over the analyzed time frame. There is no evidence of a long-term monotonic increase or decrease in the UHII during the period of observation. Trend analysis using the Mann–Kendall test was also considered, however, the relatively short duration of the dataset represents a limitation to the investigation of trends.

In more detail, the highest values of $UHII_m$ are observed at Stations 4 and 5, specifically in the area of Thessaloniki's International Fair Center (in the city center) and in the area of Kordelio (in the west side of the city), respectively. These results were reasonably expected since Station 4 is the most central station under study, while Station 5 is located in an area with few green spaces, relatively farther from the sea compared to the rest stations, near industrial sites, all raising the surface air temperature. Table 3 summarizes the highest and lowest $UHII_m$ values at each station, along with the months in which they were observed. The highest $UHII_m$ values occur at compact midrise (LCZ 2) and Large low-rise (LCZ 8) sites, peaking at 2.3 °C at Station 5. The lowest values appear in open low-rise areas (LCZ 6) at Station 2, reaching −0.6 °C. Urban morphology and land cover strongly influence these patterns (e.g., Di Sabatino et al. 2020), with dense built environments exhibiting the most intense UHI effects, while open and vegetated areas show better thermal regulation. These findings demonstrate the importance of LCZ-based urban planning for heat mitigation.

Table 3 also summarizes the negative and non-negative $UHII_m$ for each station, during the five-year period under study. At Station 1, out of the 60 months of the study, 52 months (86.7%) showcase a non-negative $UHII_m$ while there are 8 months in which $UHII_m$ is negative ranging from −0.1 to −1.1 ℃. At Station 2, out of the 57 months of measurements, 40 months (70%) demonstrate a non-negative $UHII_m$, whereas for 17 months in which $UHII_m$ is negative, the values range from −0.1 to −0.6 ℃. In Stations 3, 4, and 5, out of the 20, 53, and 56 months of measurements, respectively, all months display a non-negative $UHII_m$.

Similarly, regarding the $UHII_y$ values (Analytic data are provided in Table A1 of the Appendix), the highest one (1.5 °C) is observed at Station 5 in 2022, while the lowest one (0.1 °C) is observed at Station 2 in 2019. Notably, none of the stations exhibit a negative $UHII_y$ value. As expected, the results of $UHII_y$ agree with those of $UHII_m$. The maximum UHII values are observed at Station 5, while the minimum values are observed at Station 2 on both annual and monthly basis.

The correlation between the UHII and background temperature at the reference station varies spatially across the study

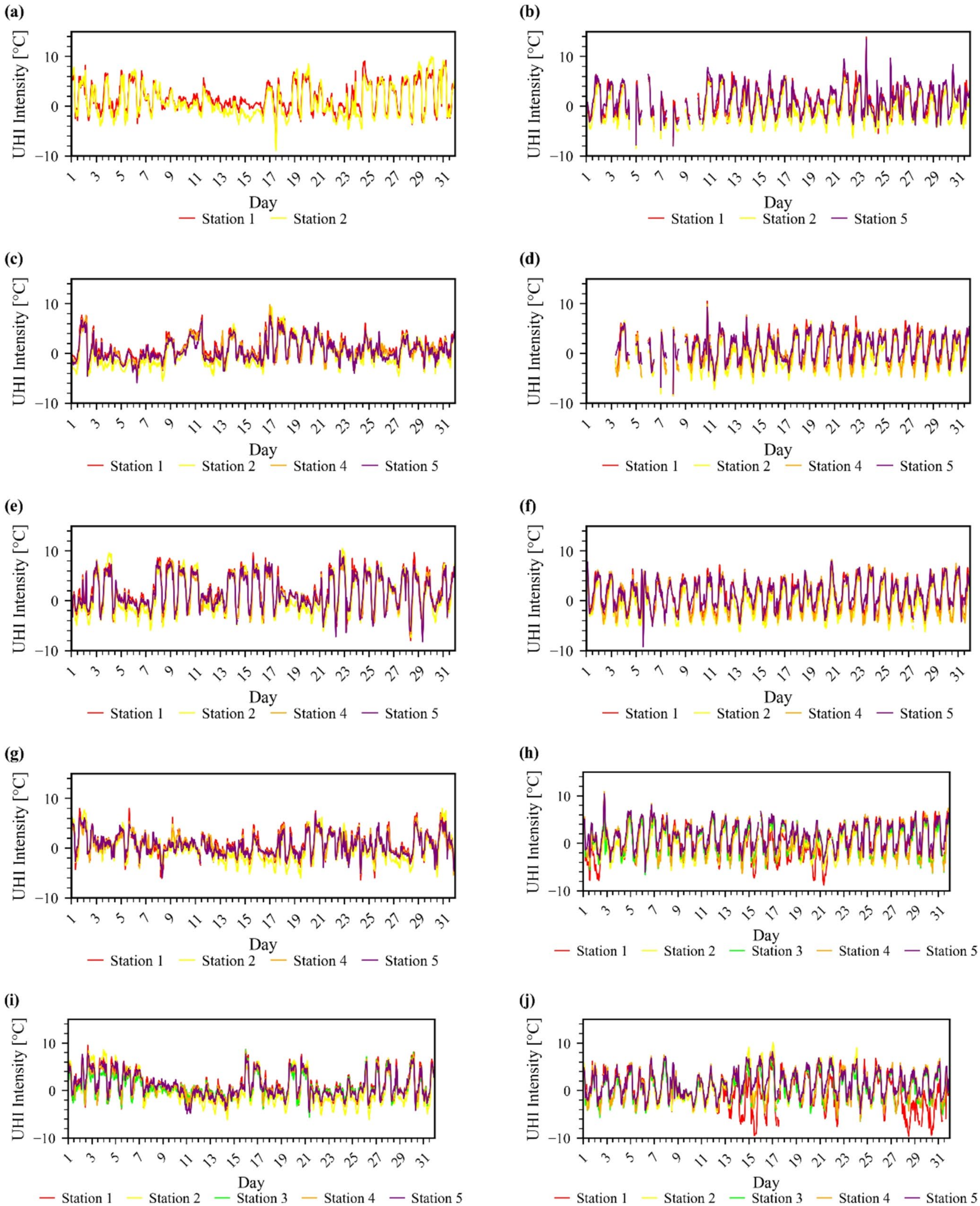

Fig. 7 $UHII_h$ pattern in January (left) and July (right) from 2018 (top) to 2022 (bottom) at the five urban meteorological stations in Thessaloniki, Greece

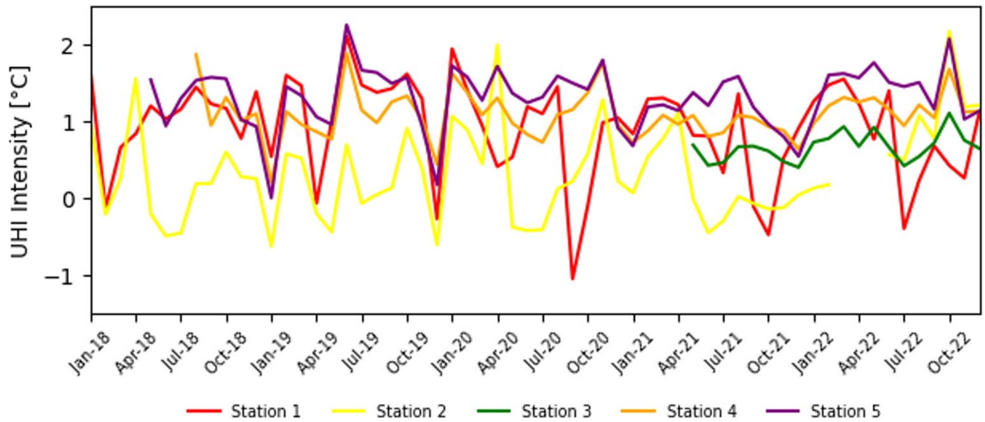

Fig. 8 $UHII_m$ pattern during 2018–2022 at the five urban meteorological stations in Thessaloniki, Greece

Table 3 $UHII_m$ compared to LCZ characteristics of the five urban meteorological stations in Thessaloniki, Greece

Station	LCZ	Built Type	Max $UHII_m$ [°C]	Min $UHII_m$ [°C]
Station 1 (MRT)	2	Compact midrise	2.1 (June-19)	−1.1 (Sep-20)
Station 2 (EPG)	6	Open low-rise	2.2 (Oct-22)	−0.6 (multiple dates)
Station 3 (KLM)	2	Compact midrise	1.1 (Oct-22)	0.4 (multiple dates)
Station 4 (HXP)	8	Large low-rise	1.9 (multiple dates)	0.2 (Jan-19)
Station 5 (KRD)	2	Compact midrise	2.3 (June-19)	0 (Jan-19)

sites, despite UHII being defined relative to the background reference, indicating that regional thermal conditions do not uniformly translate into changes in urban-rural temperature contrast. At Station 1, the negligible correlation ($r \approx -0.10$) suggests that urban and background temperatures respond similarly to regional warming and cooling, resulting in a largely stable UHII across a wide range of background temperatures. The weak negative correlations observed at Stations 2 and 3 ($r \approx -0.23$ and -0.29) indicate an inverse relationship between UHII and background temperature, whereby UHII tends to decrease as the reference temperature rises and increase as it falls. This pattern likely reflects the differential response of urban and rural surfaces to warming and cooling, including nighttime cooling dynamics and the moderating influence of vegetation cover. In contrast, the positive correlations at Stations 4 and 5 ($r \approx 0.14$ and 0.41) indicate that UHII strengthens as background temperature increases, particularly at Station 5, where urban heat storage and reduced cooling efficiency appear to amplify urban-rural thermal contrasts under warmer regimes. In spite all the correlation values are quite low, altogether these results demonstrate that UHII is largely spatially variable and governed by local surface properties and energy exchange processes rather than by background temperature alone.

Daytime and nocturnal urban heat Island intensities

To analyze the daytime and nocturnal variations (namely $UHII_{day}$ and $UHII_{night}$, respectively), a detailed evaluation was performed (Fig. 9). The $UHII_{day}$ was calculated based on the differences between the monthly average air temperature of all stations compared to the reference one during daytime (07:00–18:59), while the $UHII_{night}$ was obtained similarly during nighttime (19:00–06:59).

The results reveal that the UHI effect is more pronounced during nighttime hours compared to daytime. This occurs because urban areas retain significantly more heat than rural regions at night, as buildings and paved surfaces slowly release the thermal energy absorbed during daylight hours (Mohajerani et al. 2017). Due to their high thermal mass, these structures store warmth and minimize radiative cooling. Additionally, the dense urban landscape restricts sky visibility, trapping heat by hindering the efficient dissipation of longwave radiation (Pulvirenti and Di Sabatino 2017). All the weather stations (except for Station 5 that recorded zero values), marked a negative $UHII_{day}$, leading to the occurrence of a cool island effect in Thessaloniki.

Notably, these observed differences in UHII are strongly linked to the LCZs in which each station is located. More specifically, Station 1 is situated in a compact mid-rise urban area (LCZ 2) demonstrating consistently high nocturnal UHII values, with a peak of 2.8 °C. This is consistent with the dense built environment and limited vegetation, both of which enhance thermal storage and reduce night-time cooling. In contrast, Station 2, which is located in LCZ 6 (open low-rise area), recorded the lowest average daytime and nocturnal UHII, with −1.5 °C and 2.1 °C, respectively. The open layout, lower building density, and more permeable surfaces in LCZ 6 areas enable greater heat dissipation and limit thermal buildup, explaining the lower UHII intensities.

Stations 1, 4, and 5 recorded the highest average nocturnal UHII values, with 2.5 °C, 2.8 °C, and 2.7 °C, respectively, again reflecting their placement in highly urbanized LCZs

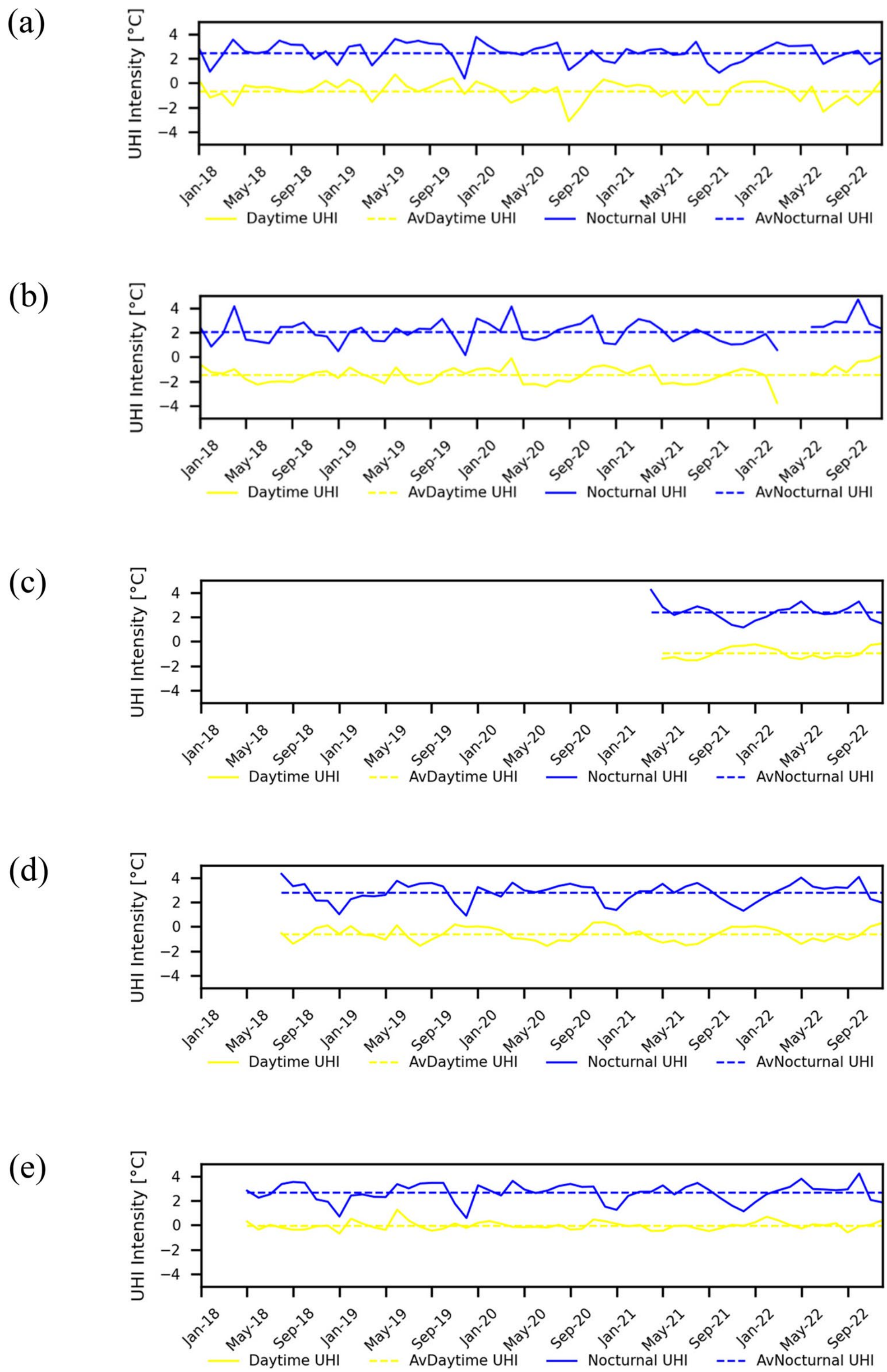

Fig. 9 $UHII_{day}$ and $UHII_{night}$ during 2018-2022 in Thessaloniki, Greece. Indices (**a**) – (**e**) correspond to stations 1–5, respectively

characterized by impervious surfaces and densely packed buildings. To better understand this contrasting phenomenon, Fig. 8 illustrates a more detailed analysis of the seasonal variations in $UHII_{day}$ and $UHII_{night}$. To this end, we compared the seasonal dispersion of UHII values during daytime and nighttime between Stations 1 and 2. These stations were selected based on two key criteria: (1) the completeness of the meteorological data provided by the respective authority to ensure robust analysis, and (2) their contrasting patterns, which offered valuable insights on the spatial and temporal dynamics of the UHI effect.

The analysis of Station 1 revealed clear seasonal trends in both nocturnal and daytime UHIIs (Fig. 10). More specifically,

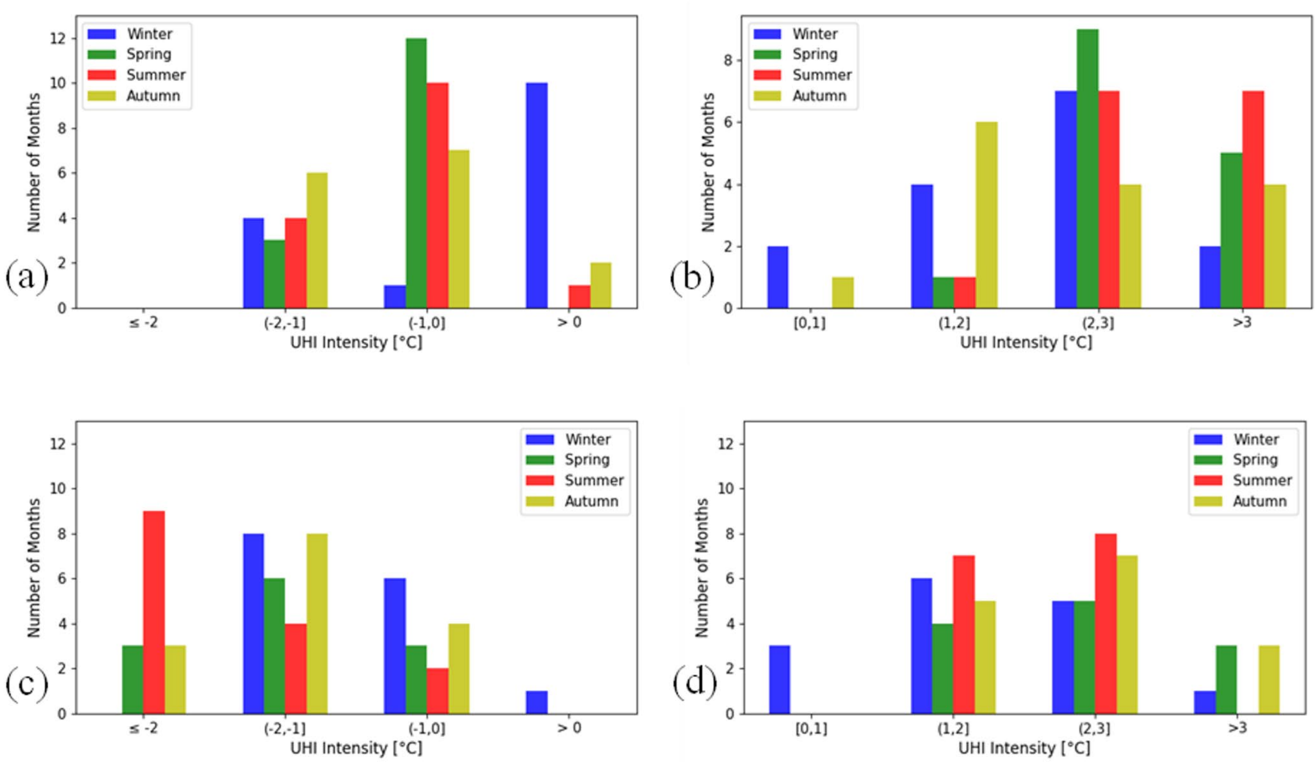

Fig. 10 Seasonal variability of $UHII_{day}$ (left) and $UHII_{night}$ (right) recorded at Station 1 (top) and Station 2 (bottom) (Note: Average values for the 2018–2022 period)

$UHII_{night}$ peaked during summer, exhibiting the highest average values among the five-year period, while winter displayed the weakest UHI effect. Spring and autumn maintained intermediate intensities, consistently exceeding 2 °C. In contrast, $UHII_{day}$ followed an inverse pattern; winter demonstrated the most prominent positive values, indicating a stronger daytime UHI effect during the colder months. The remaining seasons (spring, summer, and autumn) showed negative UHII values, suggesting that urban temperatures during daytime were cooler than those in the surrounding rural areas. This considerable dichotomy between nocturnal warming and daytime cooling highlights the complex interplay of seasonal and diurnal influences on urban microclimates.

Station 2, located in a less urbanized area than Station 1, exhibited distinct seasonal UHII patterns. During nighttime, the highest average UHII values occurred during summer and autumn, while winter showed again the weakest UHI effect. Spring demonstrated intermediate intensities, remaining above 1 °C. During daytime, winter recorded the highest positive UHII values, whereas summer produced the lowest. The remaining seasons (spring and autumn) also trended toward slightly negative UHIIs, reinforcing a weaker da time UHI effect compared to Station 1. This contrast aligns with the lower urbanization of Station 2, where reduced thermal inertia and anthropogenic heat likely dampen temperature extremes.

In summary, the clear disparities in UHII magnitude and seasonal trends between Stations 1 and 2 underscore the importance of LCZ characteristics in shaping local microclimatic conditions. Denser LCZ types (e.g., LCZ 2) show higher nocturnal UHII due to limited heat dissipation, while more open and vegetated LCZs (e.g., LCZ 9) tend to buffer temperature extremes, particularly during the day. These findings can emphasize the utility of LCZs in interpreting spatial and temporal patterns in urban heat dynamics and provide a robust framework for urban planning and climate adaptation strategies.

The impact of heatwave events on the urban heat Island

To further investigate the relationship between HWs and the UHI phenomenon, we first analyzed the extreme HW events in Thessaloniki and compared the behavior of the UHI during HW and non-HW periods (Table 4). By applying both identification methods based on the 90th percentiles of minimum and maximum daily temperatures, five distinct HW periods were identified, spanning a total of 23 days, with individual events lasting between 3 and 9 days. It should be noted that Station 3 has measurements for only 20 out of 60 months, meaning that only a subset of the detected HW days is represented, which limits the robustness of the UHII box-plot for this station.

Table 4 Metrics of heatwaves analyzed during 2018–2022 in Thessaloniki

	Number of events	Number of days	Duration of longest event	Mean normalized magnitude	Normalized magnitude of hottest day
2018	-	-	-	-	-
2019	2	7	4	3	4.4
2020	-	-	-	-	-
2021	2	13	9	6.7	9.5
2022	1	3	3	0.7	1.4

We analyzed the behavior of UHII during HW and non-HW days across five selected stations over a five-year study period. The results for daytime UHII revealed negligible variations between HW and non-HW days, as depicted in Fig. 11. Specifically, daytime UHII showed minimal changes, ranging from 0 to 0.2 °C, or even a slight reduction of up to 0.7 °C at Stations 3 and 4 during HWs.

Conversely, as illustrated in Fig. 12, nocturnal UHII exhibited an evident increase, with intensities rising by approximately 0.9 to 1.3 °C during HW events for all stations but Station 2, which recorded a change of 0.3 °C. This suggests that HW may amplify the UHI effect more significantly at night. Although the specific values varied slightly across the stations, the overall pattern remained consistent. In particular, the results confirmed an increase in nighttime UHII at all locations under study. This observed trend aligns with findings from previous research (e.g., Possega et al. 2022), reinforcing the conclusion that nocturnal UHII tends to rise during HW events. In particular, during HWs, elevated background temperatures and persistent high-pressure systems typically result in reduced wind speeds and cloud cover, both of which limit nocturnal cooling (Founda and Santamouris 2017). Urban surfaces, with their high heat storage capacity, accumulate substantial thermal energy during the day and release it slowly at night, thereby intensifying nocturnal UHII (Zhao et al. 2018). Furthermore, anthropogenic heat emissions from buildings and infrastructure may be elevated during HWs due to increased use of cooling systems, further reinforcing nighttime heat retention. Thus, the nocturnal amplification of the UHII during HWs is driven by both meteorological stagnation and urban energy balance dynamics (An et al. 2020). This finding likely suggests that thermal discomfort typical of HW events and of tropical nights, both projected to increase further in the Mediterranean area (e.g., Yavaşlı And Erlat 2024), may be significantly exacerbated for urban residents in Thessaloniki,

To assess the impact of HWs on urban heat island intensity (UHII), pairwise comparisons between non-HW (n_1) and HW (n_2) days were performed using the Mann–Whitney U test for each station and for both daytime and nighttime periods. Sample sizes reflect the relative scarcity of HW days (n_2 = 188–254) compared to normal days (n_1 = 1,971–4,899). The analysis revealed that UHII generally increased during HW periods, particularly at night, with some stations showing statistically significant differences ($p<0.05$; e.g., Station 1 and

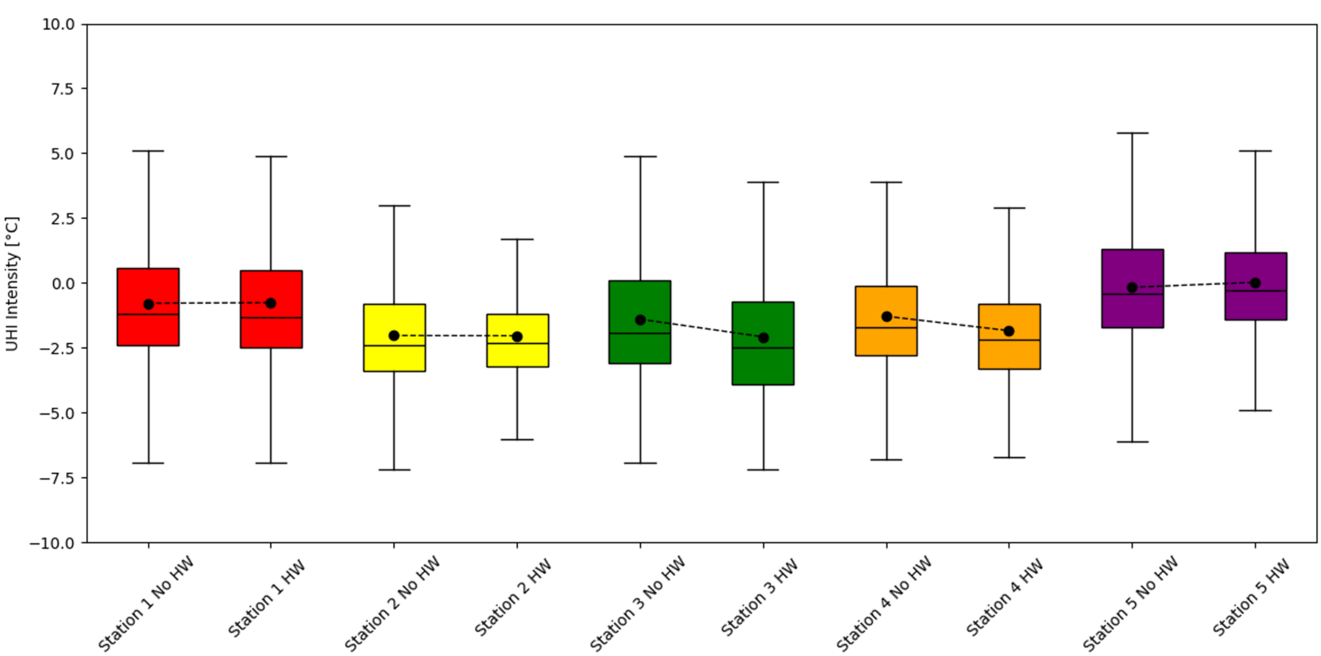

Fig. 11 Box plot analysis showing the mean variation of the $UHII_{day}$ during HW and non-HW periods

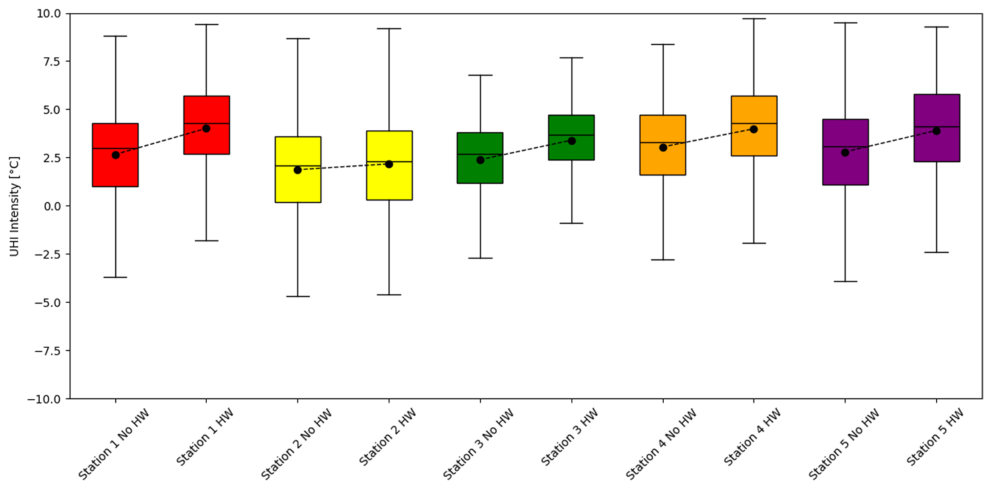

Fig. 12 Box plot analysis showing the mean variation of the $UHII_{night}$ during HW and non-HW periods

Station 5). Other stations, such as Station 3 during daytime, did not exhibit significant changes between HW and non-HW periods ($p > 0.05$), indicating heterogeneous responses across the urban sites. Moderate increases were observed at Station 2 and Station 4, with p-values close to or below 0.05 depending on the period, further highlighting that the amplification of UHII during extreme heat events is both site-specific and time-dependent. Overall, the distribution of p-values across stations and periods emphasizes the spatial and temporal heterogeneity of urban heat responses, providing quantitative evidence to inform targeted urban heat mitigation strategies.

Discussion of results

Our analysis of the urban microclimate in Thessaloniki during 2018–2022 reveals an increase in average air temperatures and UHII compared to the previous study by Giannaros and Melas (2012) conducted during 2008–2009. Specifically, the highest average air temperature in dense compact midrise LCZs (LCZ 2) rose from 17.8 °C to 18.4 °C, while peak temperatures increased from approximately 39 °C to 41 °C. The nocturnal UHII also intensified, with the maximum nocturnal UHII values reaching 2.8 °C in the recent period compared to 2.5 °C previously reported (Giannaros And Melas 2012). Moreover, the newer dataset indicates stronger diurnal and seasonal variations, including the emergence of a cold island effect during winter months, where UHII values dropped as low as −1.6 °C in less urbanized or vegetated LCZs that was not distinctly observed in the earlier study.

Both studies consistently highlight the pivotal role of LCZs in shaping UHI patterns, with densely built environments exhibiting the highest heat retention and vegetated areas contributing to localized cooling. However, the recent analysis benefits from a longer observational period and finer temporal resolution, enabling a more detailed assessment of hourly, monthly, and daytime/nocturnal temperature variations. This enhanced granularity reveals complex microclimatic interactions and more pronounced seasonal UHII fluctuations, providing deeper insights into the current urban climate challenges in Thessaloniki. The clear differentiation between LCZs also provides a practical framework for prioritizing interventions in the most heat-vulnerable districts, particularly compact mid-rise areas with limited green space. These findings underscore the need for continuous monitoring and adaptive urban planning strategies to mitigate the intensifying urban heat island effect in Mediterranean cities.

By studying Thessaloniki within the broader context of Mediterranean coastal urban climates, this study explicitly investigates regional mechanisms that influence UHI dynamics. The proximity of the sea introduces cooling daytime sea-breeze circulations while reinforcing nocturnal heat retention due to water's thermal inertia. Irregular coastal morphology and compact urban forms amplify spatial variability, with pronounced seasonal contrasts, particularly during summer HWs. Comparative evidence from other coastal cities in southern Europe such as Bari, Rome, Athens, Crete, and Barcelona shows that these coastal influences consistently shape daytime and nocturnal UHII patterns, with Thessaloniki exhibiting summer maximum UHII values exceeding 6 °C, comparable to those observed in Bari (up to 6.6 °C) (Martinelli et al. 2020) and Barcelona (up to 7 °C during winter peaks) (Martin-Vide And Moreno-Garcia 2020).

Comparable dynamics have also been reported for Lisbon, a coastal city characterized by a Mediterranean-type climate. Studies in Lisbon have shown that summertime wind regimes and breeze circulations strongly shape the intensity and timing of the UHI (Lopes et al. 2013), highlighting the close relationship between Lisbon's thermal patterns and prevailing wind conditions, while demonstrating that HWs significantly amplify the summer UHI signal and modify its daily cycle (Oliveira et al. 2021).

In addition, a broader understanding of UHII patterns can be gained by examining similar studies conducted in other Mediterranean coastal cities, such as Bari (Italy) and Barcelona

(Spain). All cities adopt comparable methodologies, using low-urbanized vegetated coastal sites as reference points for UHII estimation. Indicatively, Thessaloniki exhibits summer maximum UHII values exceeding 6 °C, with dominant nocturnal effects, while Bari records comparable peaks up to 6.6 °C and annual maximum UHII values around 2 °C. Seasonal variability is evident in both cities, often amplified during HWs, while cold-month UHI phenomena are also observed (Martinelli et al. 2020). These differences reflect the influence of local urban form, climatic conditions, and coastal proximity, highlighting the diverse dynamics of UHII across the region.

The extension of comparison to Barcelona similarly reveals significant thermal contrasts between urban and non-urban settings. An analysis of 3,285 days of minimum temperatures between the urban Barcelona-Vila Olímpica and the suburban airport station indicates that urban areas recorded higher temperatures on 91.9% of days (Martin-Vide And Moreno-Garcia 2020). The mean UHII reached 1.7 °C, increasing to 1.9 °C in the city center. Seasonal trends further underscore winter as the most intense period, with average differences of 2.7 °C and peaks up to 7.4 °C. Spring and autumn also exhibit notable UHII values of around 1.6–1.7 °C (Salvati et al. 2017). These results align with patterns observed in Thessaloniki and Bari, affirming that Mediterranean coastal cities consistently experience high UHIIs influenced by urban morphology, vegetation coverage, and atmospheric circulation patterns. This consistency across cities highlights the urgency of integrating green infrastructure, reflective materials, and permeable surfaces into urban redevelopment plans to counteract persistent nocturnal heat retention.

This approach moves beyond city-specific observations, providing new long-term evidence on how Mediterranean coastal dynamics interact with Thessaloniki's urban topography and LCZ characteristics, offering critical and fundamental insights for adaptive urban planning in coastal cities with similar conditions.

Limitations and recommendations for further investigation

This study is subject to several data- and method-related limitations. Missing observations across the five-year period and the use of only six weather stations reduce both the completeness and spatial representativeness of the dataset. The relatively short temporal window further limits the ability to assess long-term or decadal climatic trends. In addition, the absence of radiative and humidity measurements restricts the characterization of atmospheric conditions and the interpretation of UHI drivers.

A further constraint concerns the elevation difference between stations. Station 2 is located approximately 180 m higher than the suburban reference station, introducing a potential altitudinal bias in UHII estimates. Due to the lack of alternative reference stations, this discrepancy could not be corrected, and the station was retained to preserve temporal coverage. These factors highlight the need for cautious interpretation of the results.

It is important to note that the missing data, particularly the substantial gaps at Station 3 during 2018-–2020, reduces the temporal robustness of the dataset and limits the reliability of year-to-year comparisons. Analyses requiring continuous multi-year coverage were therefore restricted to stations and periods with sufficient data to minimize bias. Station 3 was nevertheless retained because it represents an LCZ type that would otherwise be absent from the spatial assessment, and excluding it would have reduced the morphological diversity captured in the study.

Future research should build on the present findings by integrating additional observational and modeling approaches. Satellite-based products (e.g., land surface temperature, vegetation indices, and surface albedo) could complement in-situ measurements and provide a spatially continuous perspective on UHI patterns across the wider metropolitan area. High-resolution numerical simulations, such as those produced with the Weather Research and Forecasting (WRF) model, would allow for a more detailed examination of the physical processes driving UHI formation (Liu et al. 2024) and could help isolate the influence of urban morphology, sea-breeze dynamics, and topographic effects.

Exploring future climate scenarios would further clarify how projected warming and changes in HW frequency may modify UHII in Mediterranean coastal cities. Coupling UHI metrics with socioeconomic indicators, such as mortality, morbidity, or energy consumption, would also provide valuable insights into the human and infrastructural impacts of urban overheating. Such interdisciplinary approaches could support more targeted adaptation strategies and strengthen the evidence base for urban planning and public-health interventions.

Conclusions

This study provides a comprehensive assessment of the UHI dynamics in Thessaloniki, offering new insights into the behavior of urban temperatures in an eastern Mediterranean coastal area. By analyzing long-term hourly temperature records from multiple urban stations and a suburban reference site, we were able to characterize both the spatial variability and the seasonal evolution of the UHI effect. Although the higher elevation of Station 2 introduces a known limitation, the dataset enabled a robust evaluation of how urban form, land cover, and climatic conditions interact to shape thermal patterns across the metro area.

The results demonstrate that Thessaloniki experiences a persistent and seasonally modulated UHI effect, with the strongest intensities occurring during nighttime and throughout the warm season. The influence of LCZs was particularly evident; compact, densely built areas consistently exhibited the highest nocturnal UHII values, whereas open, low-rise zones showed markedly weaker effects. The presence of a cool-island phenomenon during winter at certain stations where synoptic conditions and seasonal energy balances can temporarily reverse typical UHI behavior.

The study also reveals a clear interaction between HWs and the UHII in Thessaloniki. UHII was generally higher during heatwave periods than during non-HW days, particularly at night, although the magnitude and statistical significance of this increase varied across stations and between daytime and nighttime conditions. Nocturnal UHII increased substantially during HW periods, amplifying thermal stress and reducing the potential for nighttime cooling. No statistically significant long-term trends in the UHII were detected at any station during the 2018–2022 period, indicating overall stability of the UHII over the study timeframe despite short-term HW-related variability. This compounding effect underscores the vulnerability of Mediterranean cities to extreme heat and emphasizes the need for targeted adaptation strategies that address both chronic and sporadic thermal risks. The relationship between UHII and background temperature was highly site dependent, with correlations ranging from weakly negative to moderately positive, demonstrating that regional warming does not uniformly translate into changes in urban–rural thermal contrast.

From a planning perspective, the findings highlight the need to expand green infrastructure and improve surface permeability in Thessaloniki's dense, low-green urban areas. Large-scale interventions, such as the creation of a metropolitan park at the International Fair site, could provide meaningful cooling benefits, while complementary measures including cool pavements, reflective building materials, water features, and green roofs could further mitigate heat retention. Additionally, the design of ventilation corridors capable of channeling sea-breeze flows into the urban core represents a promising strategy for improving nighttime cooling in compact districts.

Overall, this study advances the understanding of the UHI processes in a Mediterranean coastal setting and highlights the need for context-specific mitigation approaches that account for local morphology, climatic conditions, and seasonal variability. The obtained insights can support evidence-based urban planning not only in Thessaloniki but also in other rapidly warming coastal cities facing similar environmental challenges.

Appendix

Table A1 Monthly average ($UHII_m$) and annual average ($UHII_y$) intensity of urban heat Island for the stations of the entire study

Station							$UHII_m$ [°C]							$UHII_y$
	Year	Jan	Feb	Mar	Apr	May	Jun	Jul	Aug	Sep	Oct	Nov	Dec	[°C]
1	2018	1.6	−0.1	0.7	0.8	1.2	1	1.2	1.4	1.2	1.2	0.8	1.4	1
	2019	0.5	1.6	1.5	−0.1	1	2.1	1.5	1.4	1.4	1.6	1.3	−0.3	1.1
	2020	1.9	1.4	0.9	0.4	0.5	1.2	1.1	1.4	−1.1	−0.1	1	1	0.8
	2021	0.8	1.3	1.3	1.2	0.8	0.8	0.3	1.4	−0.1	−0.5	0.5	0.9	0.7
	2022	1.3	1.5	1.5	1.2	0.8	1.4	−0.4	0.2	0.7	0.4	0.3	1.1	0.8
2	2018	1	−0.2	0.3	1.6	−0.2	−0.5	−0.5	0.2	0.2	0.6	0.3	0.2	0.2
	2019	−0.6	0.6	0.5	−0.2	−0.4	0.7	−0.1	0	0.1	0.9	0.4	−0.6	0.1
	2020	1.1	0.9	0.4	2	−0.4	−0.4	−0.4	0.1	0.2	0.6	1.3	0.2	0.5
	2021	0.1	0.5	0.8	1.1	0	−0.5	−0.3	0	−0.1	−0.1	−0.1	0	0.1
	2022	0.1	0.2	-	-	-	0.6	0.5	1.1	0.8	2.2	1.2	1.2	0.9
3	2018	-	-	-	-	-	-	-	-	-	-	-	-	-
	2019	-	-	-	-	-	-	-	-	-	-	-	-	-
	2020	-	-	-	-	-	-	-	-	-	-	-	-	-
	2021	-	-	-	-	0.7	0.4	0.5	0.7	0.7	0.6	0.5	0.4	0.5
	2022	0.7	0.8	0.9	0.7	0.9	0.7	0.4	0.5	0.7	1.1	0.7	0.6	0.7
4	2018	-	-	-	-	-	-	-	1.9	0.9	1.3	1	1.1	1.2
	2019	0.2	1.1	1	0.9	0.8	1.9	1.1	1	1.2	1.3	1	0.4	1
	2020	1.6	1.4	1.1	1.3	1	0.8	0.7	1.1	1.1	1.4	1.8	0.9	1.2
	2021	0.7	0.9	1.1	1	1.1	0.8	0.8	1.1	1	0.9	0.9	0.6	0.9
	2022	1	1.2	1.3	1.2	1.3	1.2	0.9	1.2	1	1.7	1.1	1.1	1.2
5	2018	-	-	-	-	1.5	0.9	1.3	1.5	1.6	1.5	1	0.9	1.3
	2019	0	1.4	1.3	1.1	1	2.3	1.7	1.6	1.5	1.6	0.9	0.2	1.2
	2020	1.7	1.6	1.3	1.7	1.4	1.2	1.3	1.6	1.5	1.4	1.8	0.9	1.4
	2021	0.7	1.2	1.2	1.1	1.4	1.2	1.5	1.6	1.2	1	0.8	0.5	1.1
	2022	1	1.6	1.6	1.6	1.8	1.5	1.4	1.5	1.2	2.1	1	1.1	1.5

Acknowledgements The authors are grateful to the Department of Environment and Climate Change Adaption of the municipality of Thessaloniki, the National Observatory of Athens, and the Hellenic National Meteorological Service for providing the meteorological data required for this study. We would also like to acknowledge Dr. Ilias Agathangelidis for developing the Hotspell Python package, used for the heatwave events' identification in this study.

Author contributions E. Christakakis: Conceptualization; Methodology; Validation; Formal analysis; Investigation; Data curation; Writing - Original Draft; Writing - Review and Editing. E. Aivazidou: Conceptualization; Validation; Writing - Original Draft; Writing - Review and Editing; Supervision. E. Brattich: Conceptualization; Methodology; Writing - Original Draft; Writing - Review and Editing; Supervision.

Funding Open access funding provided by Alma Mater Studiorum - Università di Bologna within the CRUI-CARE Agreement. The authors declare that no funds, grants, or other support were received during the preparation of this manuscript.

Data availability Data cannot be shared openly but are available on request from authors.

Declarations

Competing interests The authors declare no competing interests.

References

Acero JA, Arrizabalaga J, Kupski S, Katzschner L (2013) Urban heat island in a coastal urban area in northern Spain. Theor Appl Climatol 113:137–154. https://doi.org/10.1007/s00704-012-0774-z

An N, Dou J, González-Cruz JE, Bornstein RD, Miao S, Li L (2020) An observational case study of synergies between an intense heat wave and the urban heat island in Beijing. J Appl Meteorol Climatol 59:605–620. https://doi.org/10.1175/JAMC-D-19-0125.1

Anjos M, Lopes A (2017) Urban heat island and park cool island intensities in the coastal city of Aracaju, north-eastern Brazil. Sustainability 9:1379. https://doi.org/10.3390/su9081379

Arifwidodo S, Chandrasiri O, Abdulharis R, Kubota T (2019) Exploring the effects of urban heat island: a case study of two cities in Thailand and Indonesia. APN Sci Bull 9. https://doi.org/10.30852/sb.2019.539

Bouketta S (2023) Urban cool island as a sustainable passive cooling strategy of urban spaces under summer conditions in Mediterranean climate. Sustain Cities Soc 99:104956. https://doi.org/10.1016/j.scs.2023.104956

Di Bernardino A, Falasca S, Iannarelli AM, Casadio S (2023) Effect of heatwaves on urban sea breeze, heat island intensity, and outdoor thermo-hygrometric comfort in Rome (Italy). Urban Clim 52:101735. https://doi.org/10.1016/j.uclim.2023.101735

Di Sabatino S, Barbano F, Brattich E, Pulvirenti B (2020) The multiple-scale nature of urban heat island and its footprint on air quality in real urban environment. Atmosphere 11:1186. https://doi.org/10.3390/atmos11111186

Founda D, Santamouris M (2017) Synergies between urban heat island and heat waves in Athens (Greece), during an extremely hot summer (2012). Sci Rep 7:10973. https://doi.org/10.1038/s41598-017-11407-6

Galanaki E, Giannaros C, Kotroni V, Lagouvardos K, Papavasileiou G (2023) Spatio-temporal analysis of heatwaves characteristics in Greece from 1950 to 2020. Climate 11:5. https://doi.org/10.3390/cli11010005

Giannakopoulos C, Psiloglou B, Lemesios G et al (2016) Climate change impacts, vulnerability and adaptive capacity of the electrical energy sector in Cyprus. Reg Environ Change 16:1891–1904. https://doi.org/10.1007/s10113-015-0885-z

Giannaros TM, Melas D (2012) Study of the urban heat island in a coastal mediterranean city: the case study of Thessaloniki, Greece. Atmos Res 118:103–120. https://doi.org/10.1016/j.atmosres.2012.06.006

Giannaros TM, Melas D, Daglis IA, Keramitsoglou I, Kourtidis K (2013) Numerical study of the urban heat island over Athens (Greece) with the WRF model. Atmos Environ 73:103–111. https://doi.org/10.1016/j.atmosenv.2013.02.055

Giridharan R, Kolokotroni M (2009) Urban heat island characteristics in London during winter. Sol Energy 83:1668–1682. https://doi.org/10.1016/j.solener.2009.06.007

Hellenic Statistical Authority (2023) 2021 population census results. https://www.statistics.gr/en/2021-census-res-pop-results, Accessed 14 July 2025

Hellenic National Meteorological Service (2023) climate data. http://climatlas.hnms.gr/sdi/?lang=EN. Accessed 14 July 2025

IPCC (2023) Climate Change 2023: Synthesis Report. Contribution of Working Groups I, II and III to the Sixth Assessment Report of the Intergovernmental Panel on Climate Change. Geneva, Switzerland: IPCC. https://www.ipcc.ch/report/ar6/syr/

Keppas SC, Papadogiannaki S, Parliari D, Kontos S, Poupkou A, Tzoumaka P, Kelessis A, Zanis P, Casasanta G, Melas D (2021) Future climate change impact on urban heat island in two Mediterranean cities based on high-resolution regional climate simulations. Atmosphere 12:884. https://doi.org/10.3390/atmos12070884

Kim Y, Baik J (2005) Spatial and temporal structure of the urban heat island in Seoul. J Appl Meteorol Climatol 44:591–605. https://doi.org/10.1175/JAM2226.1

Lazoglou G, Hadjinicolaou P, Sofokleous I, Bruggeman A, Zittis G (2024) Climate change and extremes in the Mediterranean island of Cyprus: from historical trends to future projections. Environ Res Commun 6:095020. https://doi.org/10.1088/2515-7620/ad7927

Lehoczky A, Sobrino JA, Skoković D, Aguilar E (2017) The urban heat island effect in the city of valencia: a case study for hot summer days. Urban Sci 1:9. https://doi.org/10.3390/urbansci1010009

Li Y, Schubert S, Kropp JP et al (2020) On the influence of density and morphology on the urban heat island intensity. Nat Commun 11:2647. https://doi.org/10.1038/s41467-020-16461-9

Liu B, Guo X, Jiang J (2023) How urban morphology relates to the urban heat island effect: a multi-indicator study. Sustainability 15:10787. https://doi.org/10.3390/su151410787

Liu C, Lu S, Tian J, Yin L, Wang L, Zheng W (2024) Research overview on urban heat islands driven by computational intelligence. Land 13:2176. https://doi.org/10.3390/land13122176

Liu S, Wang Y et al (2025) Regional warming from urbanization is disproportionate to urban expansion rate. One Earth 8:101234. https://doi.org/10.1016/j.oneear.2025.101234
Lopes A, Alves E, Alcoforado MJ, Machete R (2013) Lisbon urban heat island updated: new highlights about the relationships between thermal patterns and wind regimes. Adv Meteorol. https://doi.org/10.1155/2013/487695
Lu S, Liu F, Ye Y et al (2024) Analysis of the spatio-temporal characteristics of winter surface urban heat island: a case study in Beijing, China. J Earth Sci 35:1640–1653. https://doi.org/10.1007/s12583-023-1880-9
Martin-Vide J, Moreno-Garcia MC (2020) Probability values for the intensity of Barcelona's urban heat island (Spain). Atmos Res 240:104877. https://doi.org/10.1016/j.atmosres.2020.104877
Martinelli A, Kolokotsa D, Fiorito F (2020) Urban heat island in mediterranean coastal cities: the case of Bari (Italy). Climate 8:79. https://doi.org/10.3390/cli8060079
Mohajerani A, Bakaric J, Jeffrey-Bailey T (2017) The urban heat island effect, its causes, and mitigation, with reference to the thermal properties of asphalt concrete. J Environ Manag 197:522–538. https://doi.org/10.1016/j.jenvman.2017.03.095
Nuruzzaman M (2015) Urban heat island: causes, effects and mitigation measures - a review. Int J Environ Monit Anal 3:67–73. https://doi.org/10.11648/j.ijema.20150302.15
Oke TR (1973) City size and the urban heat island. Atmos Environ 7:769–779. https://doi.org/10.1016/0004-6981(73)90140-6
Oke TR (1982) The energetic basis of the urban heat island. Q J R Meteorol Soc 108:1–24. https://doi.org/10.1002/qj.49710845502
Oliveira A, Lopes A, Correia E, Niza S, Soares A (2021) Heatwaves and summer urban heat islands: a daily cycle approach to unveil the urban thermal signal changes in Lisbon, Portugal. Atmosphere 12:292. https://doi.org/10.3390/atmos12030292
Pappalardo SE, Zanetti C, Todeschi V (2023) Mapping urban heat islands and heat-related risk during heat waves from a climate justice perspective: a case study in the municipality of Padua (Italy) for inclusive adaptation policies. Landsc Urban Plann 238:104831. https://doi.org/10.1016/j.landurbplan.2023.104831
Perkins SE, Alexander LV (2013) On the measurement of heat waves. J Clim 26:4500–4517. https://doi.org/10.1175/JCLI-D-12-00383.1
Possega M, Aragão L, Ruggieri P, Santo MA, Di Sabatino S (2022) Observational evidence of intensified nocturnal urban heat island during heatwaves in European cities. Environ Res Lett 17:124013. https://doi.org/10.1088/1748-9326/aca3ba
Pulvirenti B, Di Sabatino S (2017) CFD characterization of street canyon heating by solar radiation on building walls. In: proceedings of the HARMO 2017–18th international conference on harmonisation within atmospheric dispersion modeling for regulatory purposes, bologna, italy. Hungarian Meteorological Service, Budapest, Hungary, pp 902–906. https://doi.org/10.48550/arXiv.2006.04800
Salvati A, Coch Roura H, Cecere C (2017) Assessing the urban heat island and its energy impact on residential buildings in mediterranean climate: Barcelona case study. Energy Build 146:38–54. https://doi.org/10.1016/j.enbuild.2017.04.025
Santamouris M (2020) Recent progress on urban overheating and heat island research. Integrated assessment of the energy, environmental, vulnerability and health impact. Synergies with the global climate change. Energy Buildings 207:109482. https://doi.org/10.1016/j.enbuild.2019.109482
Santamouris M, Haddad S, Fiorito F, Osmond P, Ding L, Prasad D, Zhai X, Wang R (2017) Urban heat island and overheating characteristics in sydney, Australia. An analysis of multiyear measurements. Sustainability 9:712. https://doi.org/10.3390/su9050712
Silva R, Carvalho AC, Cardoso Pereira S, Carvalho D, Rocha A (2022) Lisbon urban heat island in future urban and climate scenarios. Urban Climate 44:101218. https://doi.org/10.1016/j.uclim.2022.101218
United Nations (2018) The World's Cities in 2018. https://www.un.org/en/development/desa/population/publications/pdf/urbanization/the_worlds_cities_in_2018_data_booklet.pdf. Accessed 14 July 2025
United Nations (2022) World Population Prospects – Summary of Results. https://www.un.org/development/desa/pd/sites/www.un.org.development.desa.pd/files/wpp2022_summary_of_results.pdf. Accessed 14 July 2025
Vardoulakis E, Karamanis D, Fotiadi A, Mihalakakou G (2013) The urban heat island effect in a small mediterranean city of high summer temperatures and cooling energy demands. Sol Energy 94:128–144. https://doi.org/10.1016/j.solener.2013.04.016
Voogt JA, Oke TR (2003) Thermal remote sensing of urban climates. Remote Sens Environ 86:370–384. https://doi.org/10.1016/S0034-4257(03)00079-8
World Meteorological Organization (2023) WMO climate data and monitoring. https://worldweather.wmo.int/en/home.html. Accessed 14 July 2025
Yavaşlı D, Erlat E (2024) Tropical nights in the mediterranean: a spatiotemporal analysis of trends from 1950 to 2022. Int J Climatol 44:1472–1488. https://doi.org/10.1002/joc.8394
Yun GY, Ngarambe J, Nzivugira Duhirwe P, Ulpiani G, Paolini R, Haddad S, Vasilakopoulou K, Santamouris M (2020) Predicting the magnitude and the characteristics of the urban heat island in coastal cities in the proximity of desert landforms: the case of Sydney. Sci Total Environ 709:136068. https://doi.org/10.1016/j.scitotenv.2019.136068
Zhao L, Oppenheimer M et al (2018) Interactions between urban heat islands and heat waves. Environ Res Lett. https://doi.org/10.1088/1748-9326/aa9f73